3 Surfaces and Interfaces

3-1 Structure and Phase Transition of the Si(113) Surface

Many studies have been made on clean Si surfaces. Most of these studies were focused on low-indexed surfaces such as the (001) and (111) surfaces. Recently several authors have investigated high-indexed surfaces. High-indexed surfaces have lower symmetry than the (001) and (111) surfaces, therefore it is expected that these surfaces can be a leading candidate of a stage of one-dimensional physics. It is well known that the Si(113) clean surface has a flat and stable 3×2 structure. In many studies, the Si(113) surface structure is explained by Dabrwoski's interstitial model [1, 2]. The Dabrowski model has an interstitial atom in two connected units of Ranke's 3×1 structure [3]. However, the Si(113) surface structure is not yet determined completely.

In this work [4], we have studied the Si(113) 3×1 surface with surface X-ray diffraction using synchrotron radiation at BL-15B2. We compared the experimental structure factors obtained from the integrated intensities of the fractional-order reflections with calculated structure factors using above-mentioned models. The X-rays were monochromatized at a wavelength of 0.86 Å. The grazing incident angle of the X-ray beams to the substrate was about 0.5°. The equipment consists of an ultrahigh vacuum (UHV) chamber operating at arround 5×10^{-10} Torr coupled to a 6-circle diffractometer. In addition to X-ray diffraction, the chamber has facilities for reflection high energy electron diffraction (RHEED). The sample was cleaned by indirect heating of the substrate to 1090 °C in the UHV chamber, then slowly cooled to room temperature. This results in sharp Si(111) 3×1 RHEED patterns.

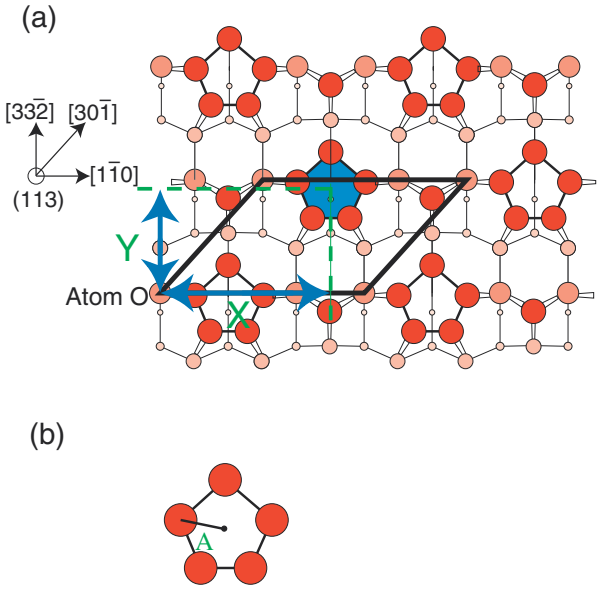

Figure 1
(a) A schematic illustration of the 3×1 dimerized structure model of Ranke. Solid lines indicate the 3×1 unit cell. The origin of X, Y is shown as an atom O. (b) The pentagon of the model, in which the size of the pentagon is defined.

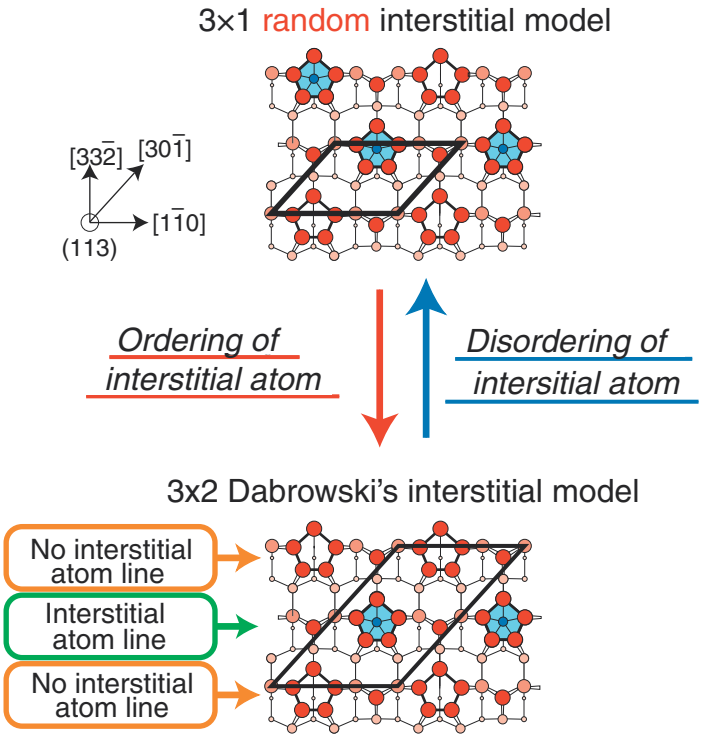

Figure 2
The model for the 3×1 ↔ 3×2 phase transition.

We measured a total of 120 different reflections, of which 45 were non-equivalent. The measured intensity profiles had a Lorentzian line shape and the integrated intensities were obtained from curve fitting.

Observed structure factors were obtained from the integrated intensities. Several structure models for the 3×1 structure have been proposed based on a dimerized structure model [3] originally proposed by Ranke as shown in Fig. 1(a). The essential feature of the 3×1 dimerized structure model is a pentagon of Si atoms. We determined the center position (X, Y) and the size (A) of the pentagon as shown in Fig. 1 using a reliability factor (R-factor). We assumed that the pentagon is equilateral. By minimizing the R-factor, we obtained the position of its center X, Y and its size A. The obtained values of the parameters X, Y, and A are 9.53 ± 0.2 Å, 5.53 ± 0.2 Å, and 1.94 ± 0.1 Å. Using these parameters, the R-factor has a minimum value of 0.277.

It is well known that there is a 3×1 ↔ 3×2 phase transition on the Si(113) surface. For the 3×2 structure on the Si(113) surface, Dabrowski's structural model was proposed, in which an interstitial Si atom exists in the center of the pentagon alternately to form a 3×2 unit. The 3×1 structure can be thought to be a superposition of small domains of the 3×2 structure with antiphase boundaries, as has been observed using scanning tunneling microscope. As the limit of small domain size, we have considered a model for the 3×1 structure with randomly distributed interstitial atoms at the center of the pentagons. Using this model with 40% site occupancy of randomly distributed interstitial atoms, the R-factor has a smaller value of 0.265. This result supports an ordering-disordering mechanism for the 3×1 ↔ 3×2 phase transition as shown in Fig. 2.

Y. Mizuno[1], K. Akimoto[1], T. Aoyama[1], H. Suzuki[1], H. Nakahara[1], A. Ichimiya[1], K. Sumitani[2] and T. Takahashi[2] ([1]Nagoya Univ., [2]Univ. of Tokyo)

References

[1] J. Dabrowski, H. J. Müssig and G. Wolff, *Phys. Rev. Lett.,* **73** (1994) 1660.
[2] J. Dabrowski, H.-J. Müssig and G. Wolff, *Surf. Sci.,* **331-333** (1995) 1022.
[3] W. Ranke, *Phys. Rev. B,* **41** (1990) 5243.
[4] Y. Mizuno, K. Akimoto, T. Aoyama, H. Suzuki, H. Nakahara, A. Ichimiya, K. Sumitani, T. Takahashi, X. Zhang, H. Sugiyama and H. Kawata, *Appl. Surf. Sci.,* **237** (2004) 40.

3-2 An In-situ Photoemission Study of the Room Temperature Ferromagnet $ZnGeP_2$:Mn

After the successful synthesis of the III-V-based ferromagnetic diluted magnetic semiconductors (DMS's) $In_{1-x}Mn_xAs$ and $Ga_{1-x}Mn_xAs$ (T_C < 110 K: Curie temperature), the search for new DMS's which show higher T_C's has been one of the most important subjects in the field of "spintronics", where the integrated use of the spin degrees of freedom in semiconductor devices is envisaged. Recently, Medvedkin *et al.* discovered a new class of room-temperature ferromagnets $CdGeP_2$:Mn and $ZnGeP_2$:Mn, in which a high concentration of Mn ions (far beyond the solubility limit in III-V-based DMS's) were incorporated in the surface region of the II-IV-V_2 chalcopyrite-type semiconductors [1]. This discovery stimulated many studies ranging from the chemical stability of Mn in the II-IV-V_2 host to the origin of the ferromagnetism [2].

The Mn-doped chalcopyrites originally synthesized by Medvedkin *et al.* [1] were prepared under a thermal non-equilibrium condition, that is, a concentration gradient of Mn was present in the interfacial region. Several questions remain open; what is the depth profile of the interfacial compounds; which part of the interface is ferromagnetic; and what are the chemical and electronic states of the Mn ions. In order to characterize the interfacial compound $ZnGeP_2$:Mn, we have studied *in-situ* prepared $ZnGeP_2$:Mn by photoemission spectroscopy at BL-18A [3]. A depth profile analysis of the interfacial region was performed by mechanically thinning the sample using Ar-ion sputtering (Fig. 3). Figs. 4a and 4b show the Mn 2*p* core-level photoemission spectra and the valence-band photoemission spectra in the Mn 3*p*-3*d* excitation region, recorded at a series of times during Ar-ion sputtering on $ZnGeP_2$:Mn (nominal Mn thickness 150 Å deposited on the 400°C-annealed substrate). One can see in Fig. 4(a) that, in the shallow region (d < 500 Å), the Mn $2p_{3/2}$ peak at E_B = 639 eV and its line shape clearly indicate that a metallic Mn compound is formed. However, in the deeper region (d > 500 Å), the Mn $2p_{3/2}$ peak is shifted to E_B = 642 eV, indicating that the Mn ions are incorporated in the $ZnGeP_2$ matrix with a higher oxidization state.

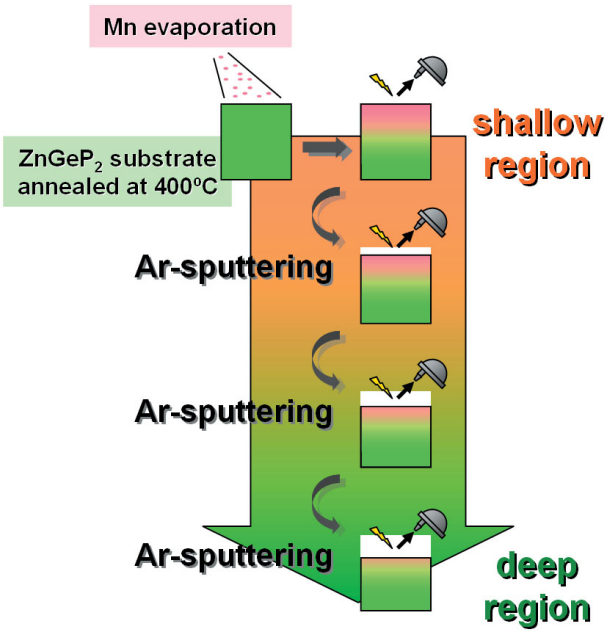

Figure 3
Synthesis and depth profile analysis of $ZnGeP_2$:Mn.

Correspondingly, the decay process following the Mn 3*p*-3*d* core excitation changes from an Auger process [Fig. 4(b-i,ii)] to a super-Coster-Krönig decay process [Fig. 4(b-iii,iv)] when going into the deeper region, indicating that the Mn 3*d* electrons change their character from itinerant to localized in the deep region. The difference spectra between the on- ($h\nu$= 51 eV) and off-resonance ($h\nu$ = 48 eV) in the deep region peaks at E_B ~ 4 eV, which is similar to those observed in the prototypical ferromagnetic DMS $Ga_{1-x}Mn_xAs$ [4]. Therefore, in the deep region, Mn ions are likely to be divalent under the tetrahedral coordination. We have also performed magnetization measurements and confirmed the room temperature ferromagnetism even after removing the metallic Mn compound. Our study suggests that the dilute divalent Mn ions, most likely in the substitutional sites of the cations in $ZnGeP_2$, are responsible for the room-temperature ferromagnetism in $ZnGeP_2$:Mn.

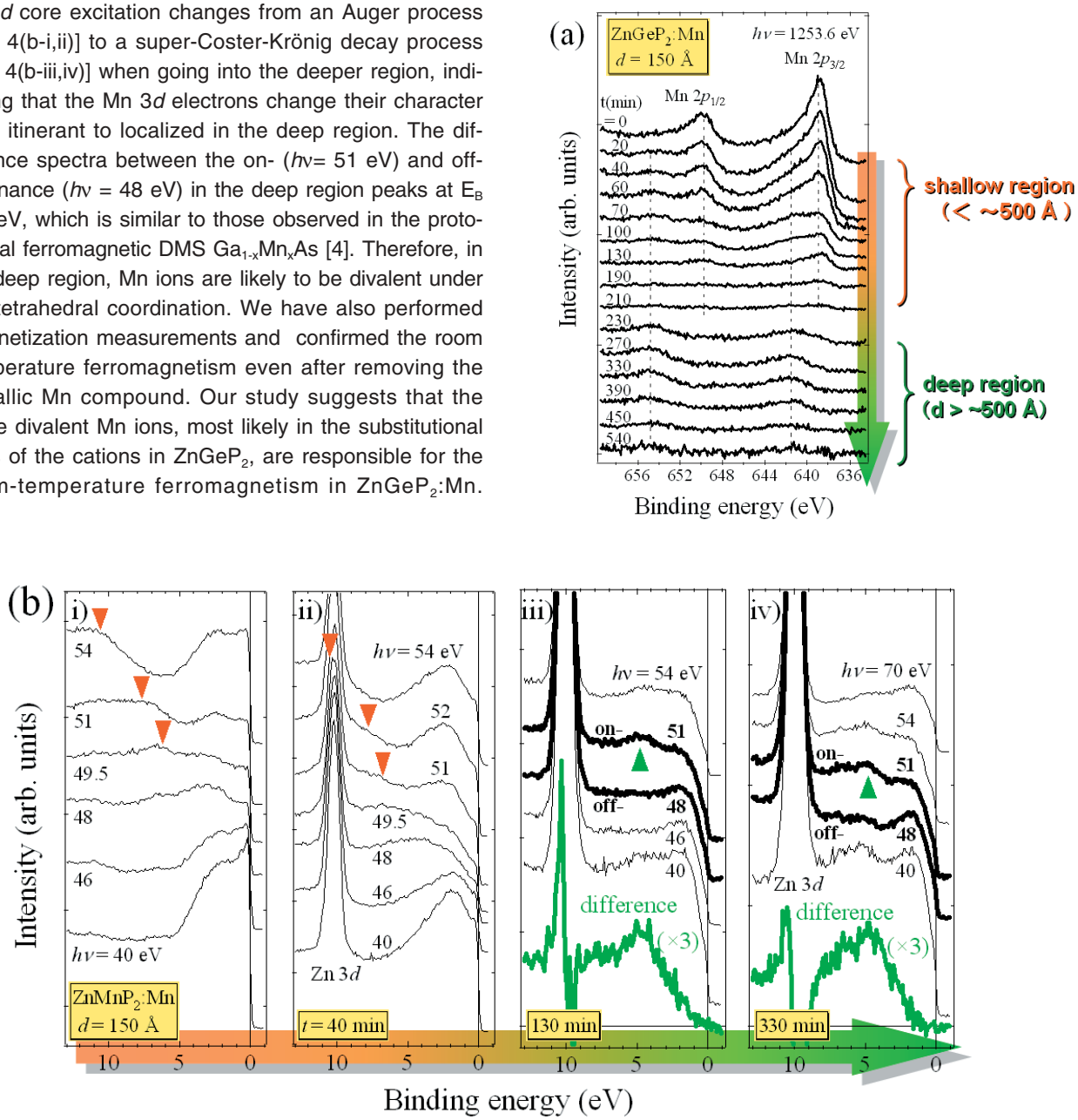

Figure 4
Depth profile series of $ZnGeP_2$:Mn. (a) Mn 2*p* core-level photoemission spectra. (b) Valence-band photoemission spectra. Orange and green triangles indicate the Mn $M_{2,3}M_{4,5}M_{4,5}$ Auger peak and the resonantly enhanced Mn 3*d*-derived peak, respectively. The sputtering rate was ~2 Å/min.

Y. Ishida[1], D.D. Sarma[2,1], K. Okazaki[1], J. Okabayashi[1], J.I. Hwang[1], H. Ott[3], A. Fujimori[1], G.A. Medvedkin[4,5], T. Ishibashi[5] and K. Sato[5] ([1]Univ. of Tokyo, [2]Indian Institute of Science, [3]Freie Univ. Berlin, [4]Ioffe Physico-Technical Institute, [5]Tokyo Univ. of Agri. & Tech.)

References

[1] G.A. Medvedkin, T. Ishibashi, T. Nishi, K. Hayata, Y. Hasegawa and K. Sato, *Jpn. J. Appl. Phys.,* **39** (2000) L949.

[2] P. Mahadevan and A. Zunger, *Phys. Rev. Lett.,* **88** (2002) 047205; Y.-J. Zhao, S. Picozzi, A. Continenza, W. T. Geng and A. J. Freeman, *Phys. Rev. B,* **65** (2002) 094415; T. Kamatani and H. Akai, *Phase Transit.,* **76** (2003) 401; S.C. Erwin and I. Žutic, *Nature mater.,* **3** (2004) 410.

[3] Y. Ishida, D.D. Sarma, K. Okazaki, J. Okabayashi, J.I. Hwang, H. Ott, A. Fujimori, G.A. Medvedkin, T. Ishibashi and K. Sato, *Phys. Rev. Lett.,* **91** (2003) 107202.

[4] J. Okabayashi, A. Kimura, T. Mizokawa, A. Fujimori, T. Hayashi and M. Tanaka, *Phys. Rev. B,* **59** (1999) R2486.